# High-Resolution Solution Structure of the Double Cys₂His₂ Zinc Finger from the Human Enhancer Binding Protein MBP-1[†,‡]

James G. Omichinski,[§] G. Marius Clore,*[,§] Mark Robien,[§] Kazuyasu Sakaguchi,[∥] Ettore Appella,[∥] and Angela M. Gronenborn*[,§]

*Laboratory of Chemical Physics, Building 2, National Institute of Diabetes and Digestive and Kidney Diseases, and Laboratory of Cell Biology, Building 37, National Cancer Institute, National Institutes of Health, Bethesda, Maryland 20892*

*Received November 19, 1991; Revised Manuscript Received January 10, 1992*

ABSTRACT: The high-resolution three-dimensional structure of a synthetic 57-residue peptide comprising the double zinc finger of the human enhancer binding protein MBP-1 has been determined in solution by nuclear magnetic resonance spectroscopy on the basis of 1280 experimental restraints. A total of 30 simulated annealing structures were calculated. The backbone atomic root-mean-square distributions about the mean coordinate positions are 0.32 and 0.33 Å for the N- and C-terminal fingers, respectively, and the corresponding values for all atoms, excluding disordered surface side chains, are 0.36 and 0.40 Å. Each finger comprises an irregular antiparallel sheet and a helix, with the zinc tetrahedrally coordinated to two cysteines and two histidines. The overall structure is nonglobular in nature, and the angle between the long axes of the helices is 47 ± 5°. The long axis of the antiparallel sheet in the N-terminal finger is approximately parallel to that of the helix in the C-terminal finger. Comparison of this structure with the X-ray structure of the Zif-268 triple finger complexed with DNA indicates that the relative orientation of the individual zinc fingers is clearly distinct in the two cases. This difference can be attributed to the presence of a long Lys side chain in the C-terminal finger of MBP-1 at position 40, instead of a short Ala or Ser side chain at the equivalent position in Zif-268. This finding suggests that different contacts may be involved in the binding of the zinc fingers of MBP-1 and Zif-268 to DNA, consistent with the findings from methylation interference experiments that the two fingers of MBP-1 contact 10 base pairs, while the three fingers of Zif-268 contact only 9 base pairs.

Over the last few years, the human enhancer binding protein MBP-1[1] (Singh et al., 1988; Baldwin et al., 1990), also known as PRDII-BF1 (Fan & Maniatis, 1990) and HIV-EP1 (Maekawa et al., 1990; Clark et al., 1990), has been shown to play an important role in the regulation of a number of genes, exhibiting specific binding to the enhancer regions of the MHC H2-K[b] and immunoglobulin κ genes, to the virus-inducible element PRDII of the human interferon β gene promoter, and to a DNA sequence within the long terminal repeats of the HIV-1 genome. MBP-1 contains two widely separated pairs (Fan & Maniatis, 1990) of classical Cys₂His₂ zinc fingers (Miller et al., 1985; Brown et al., 1985; Klug & Rhodes, 1987; Gibson et al., 1988; Berg, 1990), each of which is capable of recognizing identical DNA sequences with similar affinities (Fan & Maniatis, 1990; Baldwin et al., 1990; Maekawa et al., 1989; Clark et al., 1990). Recently, we have shown that a synthetic 57-residue double zinc finger peptide from MBP-1 exhibits the same binding specificity and relative affinity as that observed for the intact protein (Sakaguchi et al., 1991). In this paper, we present the determination of the three-dimensional solution structure of the synthetic 57-residue double zinc finger of MBP-1 by NMR spectroscopy. While the structures of a number of single Cys₂His₂ zinc fingers have been determined in solution (Parraga et al., 1988; Lee et al.,

1989; Omichinski et al., 1990; Klevitt et al., 1990; Xu et al., 1991; Kochoyan et al., 1991a–c), preliminary resonance assignments have been obtained on a double zinc finger of SW15 (Neuhaus et al., 1990), and the structure of the complex of the triple Cys₂His₂ zinc finger of Zif-268 with DNA has been solved by X-ray crystallography (Pavletich & Pabo, 1991), the present work represents the first solution structure of a multiple Cys₂His₂ zinc finger.

## EXPERIMENTAL PROCEDURES

*Sample Preparation.* The synthesis, purification, and DNA binding properties of the double zinc finger peptide of MBP-1 have been described by Sakaguchi et al. (1991), and its amino acid sequence is KYICEECGIR(Abu)-KKPSMLKKHIRTHTDVRPYHCTYCNFSFKTKGN-LTKHMKSKAHSKK. The Abu replaces a Cys in the native protein which is not coordinated to zinc. This substitution has no effect on DNA binding but increases the stability of the peptide by removing a reactive sulfydryl which has the potential to form an intermolecular disulfide bond (Sakaguchi et al., 1991). Samples for NMR spectroscopy contained 1.8 mM peptide in the presence of 4.0 mM zinc chloride, pH 6,

[1] Abbreviations: MBP-1, major histocompatibility complex enhancer binding protein 1, also known as HIV-EP1 (human immunodeficiency virus type I enhancer binding protein) and PRDII-BF1 (positive regulatory domain II of the human interferon-β promoter binding factor 1); NMR, nuclear magnetic resonance; NOE, nuclear Overhauser effect; NOESY, two-dimensional nuclear Overhauser enhancement spectroscopy; P.COSY, two-dimensional primitive correlated spectroscopy; PE.COSY, two-dimensional primitive exclusive correlated spectroscopy; HOHAHA, two-dimensional homonuclear Hartmann–Hahn spectroscopy; 2D, two dimensional; 3D, three dimensional; rms, root mean square; SA, simulated annealing; Abu, α-aminobutyric acid.

Table I: Proton Resonance Assignments of the MBP-1 Double Zinc Finger at 25 °C and pH 6[a]

| residue | NH | C$^\alpha$H | C$^\beta$H | others |
|---|---|---|---|---|
| Lys-1 | – | 4.28 | 2.02, 1.04 | C$^\gamma$H 1.98, 1.98; C$^\delta$H 1.56, 1.56; C$^\epsilon$H 3.00, 3.00 |
| Tyr-2 | 8.46 | 4.62 | 2.93, 2.86* | C$^\delta$H 7.01; C$^\epsilon$H 6.83 |
| Ile-3 | 8.17 | 4.77 | 1.56 | C$^\gamma$H 1.25, 0.84; C$^{\gamma m}$H 0.68; C$^\delta$H 0.74 |
| Cys-4 | 8.82 | 4.46 | 3.19*, 2.64 | |
| Glu-5 | 9.45 | 4.08 | 2.13*, 2.05 | C$^\gamma$H 2.40, 2.34 |
| Glu-6 | 8.66 | 4.23 | 1.53, 1.39* | C$^\gamma$H 1.85, 1.71 |
| Cys-7 | 8.14 | 5.11 | 3.35*, 2.74 | |
| Gly-8 | 8.21 | 4.17, 3.74 | | |
| Ile-9 | 7.72 | 7.07 | 1.63 | C$^\gamma$H 1.23; C$^{\gamma m}$H 0.48; C$^\delta$H 0.44 |
| Arg-10 | 8.07 | 4.99 | 1.68, 1.64* | C$^\gamma$H 1.48, 1.48; V$^\delta$H 3.12, 3.12; N$^\epsilon$H 7.21 |
| Abu-11 | 8.70 | 4.63 | 1.82*, 1.48 | C$^\gamma$H 0.68 |
| Lys-12 | 8.67 | 4.24 | 1.94*, 1.86 | C$^\gamma$H 1.46, 1.46; C$^\delta$H 1.55, 1.55; C$^\epsilon$H 2.99, 2.99 |
| Lys-13 | 7.12 | 4.76 | 2.00, 1.58* | C$^\gamma$H 1.72, 1.43; C$^\delta$H 1.67, 1.67; C$^\epsilon$H 2.95, 2.95 |
| Pro-14 | – | 3.70 | 2.15*, 1.67 | C$^\gamma$H 2.08, 1.92; C$^\delta$H 3.65, 3.27 |
| Ser-15 | 8.37 | 4.06 | 3.91, 3.87* | |
| Met-16 | 6.87 | 4.37 | 2.23*, 2.13 | C$^\gamma$H 2.70, 2.60; C$^\epsilon$H 2.15 |
| Leu-17 | 7.55 | 4.17 | 2.06*, 1.20 | C$^\gamma$H 1.76; C$^\delta$H 0.96*, 0.86 |
| Lys-18 | 8.10 | 3.94 | 1.83, 1.83 | C$^\gamma$H 1.39, 1.39; C$^\delta$H 1.52, 1.52; C$^\epsilon$H 2.93, 2.93 |
| Lys-19 | 7.37 | 3.97 | 1.88, 1.88 | C$\gamma$H 1.41, 1.41; C$^\delta$H 1.54, 1.54; C$^\epsilon$H 3.00, 3.00 |
| His-20 | 8.02 | 4.27 | 3.48*, 3.27 | C$^{\delta 2}$H 6.93; C$^{\epsilon 1}$H 7.79 |
| Ile-21 | 8.88 | 3.58 | 2.03 | C$^\gamma$H 1.86, 1.62; C$^{\gamma m}$H 1.17; C$^\delta$H 1.02 |
| Arg-22 | 7.11 | 4.99 | 1.95*, 1.88 | C$^\gamma$H 1.86, 1.70; C$^\delta$H 3.21, 3.21; N$^\epsilon$H 7.35 |
| Thr-23 | 7.68 | 4.13 | 4.02 | C$^\gamma$H 1.18 |
| His-24 | 7.30 | 4.27 | 3.23, 3.23 | C$^{\delta 2}$H 6.64; C$^{\epsilon 1}$H 7.96 |
| Thr-25 | 7.93 | 4.26 | 4.42 | C$^\gamma$H 1.20 |
| Asp-26 | 8.34 | 4.61 | 2.68*, 2.59 | |
| Val-27 | 7.84 | 4.02 | 2.08 | C$^\gamma$H 1.20, 0.90* |
| Arg-28 | 8.25 | 4.56 | 1.60, 1.49* | C$^\gamma$H 1.33, 1.27; C$^\delta$H 3.15, 3.05; N$^\epsilon$H 7.25 |
| Pro-29 | – | 3.73 | 1.82, 1.62* | C$^\gamma$H 2.31, 2.04; C$^\delta$H 3.83, 3.65 |
| Tyr-30 | 7.71 | 4.64 | 2.95*, 2.76 | C$^\delta$H 6.95; C$^\epsilon$H 6.85 |
| His-31 | 9.00 | 5.08 | 3.24*, 3.08 | C$^{\delta 2}$H 7.15; C$^{\epsilon 1}$H 8.58 |
| Cys-32 | 8.75 | 4.67 | 3.41*, 2.88 | |
| Thr-33 | 8.55 | 4.17 | 3.71 | C$^\gamma$H 1.05 |
| Tyr-34 | 9.26 | 4.51 | 2.80*, 1.95 | C$^\delta$H 6.92; C$^\epsilon$H 6.78 |
| Cys-35 | 8.15 | 4.88 | 3.16, 2.98* | |
| Asn-36 | 8.10 | 4.77 | 3.02, 2.83* | N$^\delta$H 7.53, 6.80* |
| Phe-37 | 8.37 | 4.48 | 2.74*, 2.51 | C$^\delta$H 7.07; C$^\epsilon$H 7.37; C$^\zeta$H 7.34 |
| Ser-38 | 7.86 | 5.08 | 3.43, 3.43[b] | |
| Phe-39 | 8.83 | 4.84 | 3.40*, 2.75 | C$^\delta$H 7.25; C$^\epsilon$H 6.97; C$^\zeta$H 6.28 |
| Lys-40 | 9.54 | 4.47 | 2.11, 2.02* | C$^\gamma$H 1.66, 1.66; C$^\delta$H 1.79, 1.79; C$^\epsilon$H 2.93, 2.93 |
| Thr-41 | 7.25 | 4.75 | 4.44 | C$^\gamma$H 1.20 |
| Lys-42 | 8.41 | 3.11 | 1.61*, 1.28 | C$^\gamma$H 1.07, 1.07; C$^\delta$H 1.17, 1.17; C$^\epsilon$H 2.98, 2.98 |
| Gly-43 | 8.58 | 3.80, 3.71 | | |
| Asn-44 | 7.68 | 4.47 | 2.98, 2.84* | N$^\delta$H 7.74, 7.17 |
| Leu-45 | 7.20 | 3.21 | 2.05*, 1.26 | C$_\gamma$H 1.50; C$^\delta$H 1.05*, 1.03 |
| Thr-46 | 8.66 | 3.72 | 4.16 | C$^\gamma$H 1.18 |
| Lys-47 | 7.73 | 3.86 | 1.80, 1.80 | C$^\gamma$H 1.51, 1.36; C$^\delta$H 1.65, 1.65; C$^\epsilon$H 2.93, 2.93 |
| His-48 | 7.45 | 4.27 | 3.26*, 2.88 | C$^{\delta 2}$H 7.27; C$^{\epsilon 1}$H 7.75 |
| Met-49 | 8.55 | 4.07 | 2.30, 2.21* | C$^\gamma$H 2.94, 2.86; C$^\epsilon$H 2.13 |
| Lys-50 | 7.66 | 4.29 | 1.95*, 1.63 | C$^\gamma$H 1.56, 1.56; C$^\delta$H 1.44, 1.44; C$^\epsilon$H 2.91, 2.91 |
| Ser-51 | 7.46 | 4.42 | 4.31, 4.31 | |
| Lys-52 | 8.33 | 4.17 | 1.62, 1.62 | C$^\gamma$H 1.29, 1.29; C$^\delta$H, 1.74, 1.74; C$^\epsilon$H 2.92, 2.92 |
| Ala-53 | 7.81 | 3.93 | 0.89 | |
| His-54 | 7.65 | 4.74 | 3.34, 2.72* | C$^{\delta 2}$H 6.44; C$^{\epsilon 1}$H 7.76 |
| Ser-55 | 7.83 | 4.38 | 3.80, 3.80 | |
| Lys-56 | 8.39 | 4.33 | 1.86*, 1.75 | C$^\gamma$H 1.44, 1.44; C$^\delta$H 1.67, 1.67; C$^\epsilon$H 2.97, 2.97 |
| Lys-57 | 7.95 | 4.14 | 1.80, 1.70 | C$^\gamma$H 1.38, 1.38; C$^\delta$H 1.68, 1.68; C$^\epsilon$H 2.97, 2.97 |

[a] Chemical shifts are reported relative to 4,4-dimethyl-4-silapentane-1-sulfonate. Stereospecific assignments are denoted as follows: for the C$^\beta$ methylene protons, the asterisk indicates the H$^{\beta 3}$ proton; for the NH$_2$ protons of Asn, the asterisk indicates the H$^{\delta 21}$ proton that is cis to C$^\beta$; for the methyl protons of Val and Leu, the asterisk refers to the C$^{\gamma 1}$ and C$^{\delta 1}$ methyl groups, respectively. [b] At 15 °C the two $\beta$-methylene protons of Ser-28 are no longer degenerate and have shifts of 3.46 and 3.43 for the H$^{\beta 2}$ and H$^{\beta 3}$ protons, respectively.

in either 99.996% D$_2$O or 90% H$_2$O/10% D$_2$O.

*NMR Spectroscopy.* All spectra of the double zinc finger of MBP-1 were recorded on a Bruker AM600 spectrometer in the pure-phase absorption mode (Ernst et al., 1987). The $^1$H-NMR spectrum was assigned using conventional 2D NMR methodology (Wüthrich, 1986, 1989; Clore & Gronenborn, 1987, 1989). Spin systems were assigned using P.COSY (Marion & Bax, 1988), PE.COSY (Mueller, 1987), and HOHAHA (Bax, 1989) spectroscopy to demonstrate direct and relayed through-bond connectivities, while NOESY (Jeener et al., 1979) spectroscopy was used to identify through-space (<5 Å) interactions. To help resolve ambigu-

ities in NOE assignments, spectra were recorded at 8, 15, and 25 °C. $^3J_{HN\alpha}$ and $^3J_{\alpha\beta}$ coupling constants were measured from P.COSY spectra in H$_2$O and PE.COSY spectra in D$_2$O, respectively. The apparent $^3J_{HN\alpha}$ coupling constants measured from the splittings of the NH–C$^\alpha$H cross-peaks in the P.COSY spectrum were corrected for line width as described by Omichinski et al. (1990). An example of the quality of the NOESY spectra is shown in Figure 1, which displays the NH($F_2$ axis)–NH($F_1$ axis) and NH($F_2$ axis)–aliphatic($F_1$ axis) regions of a spectrum recorded in 90% H$_2$O/10% D$_2$O at 25 °C. A summary of the complete resonance assignments is presented in Table I.
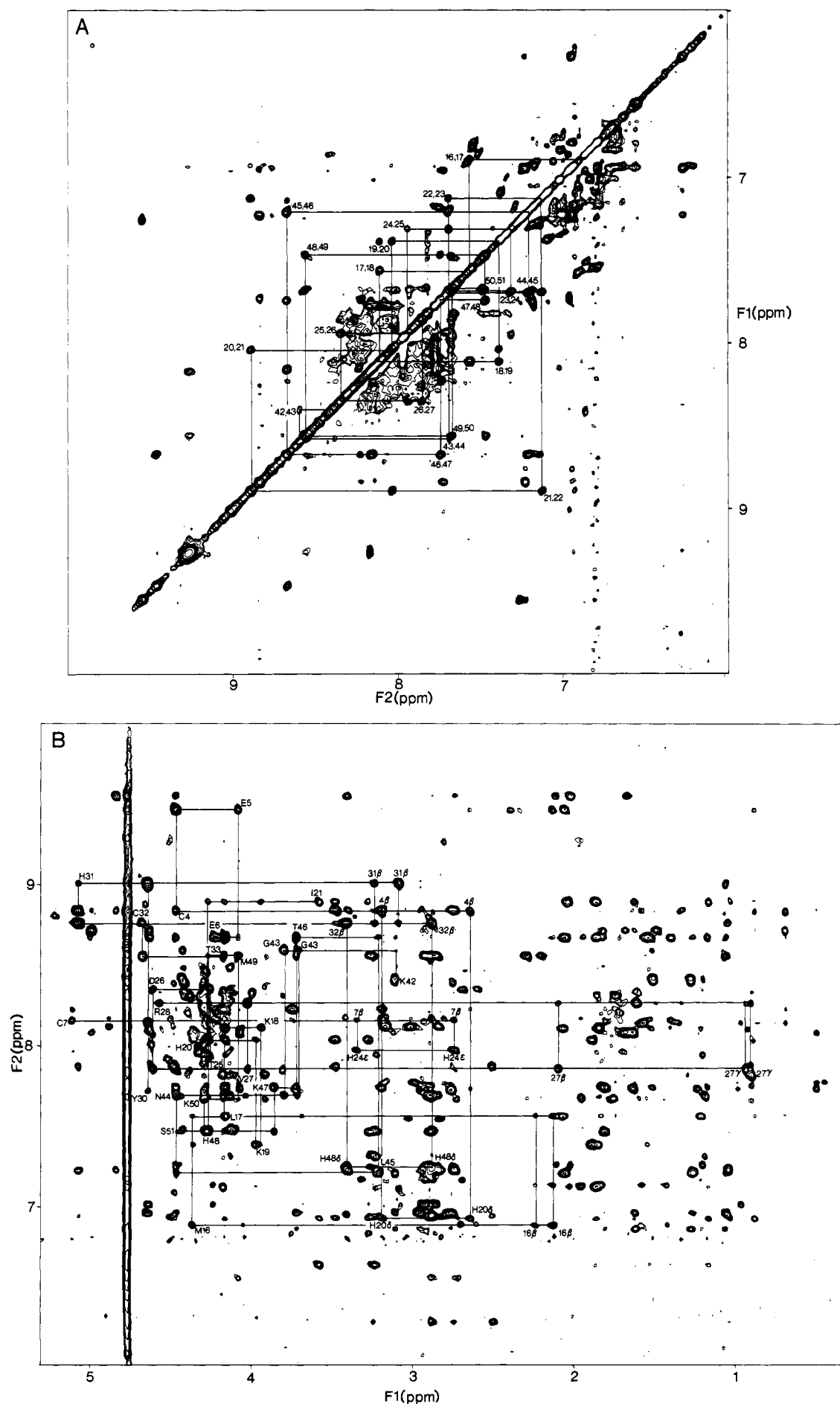
FIGURE 1: (A) NH($F_2$ axis)–NH($F_1$ axis) and (B) NH($F_2$ axis)–aliphatic($F_1$ axis) regions of the 600-MHz NOESY spectrum (150-ms mixing time) of the MBP-1–zinc complex (1.8 mM peptide, 4 mM zinc chloride) recorded in 90% $H_2O$/10% $D_2O$ at 25 °C and pH 6. A series of NH($i$)–NH($i$+1) and $C^\alpha$H($i$)–NH($i$+1) sequential NOEs are indicated in (A) and (B), respectively. Also shown in (B) are a few $C^\beta$H($i$)–NH($i$+1) NOEs as well as some long-range NOEs.

*Structure Determination.* Approximate interproton distance restraints were obtained from NOESY spectra recorded at mixing times of 50, 100, and 150 ms and classified into four ranges, 1.8–2.7, 1.8–3.3 (1.8–3.5 Å for distances involving NH protons), 1.8–5.0, and 1.8–6.0 Å, corresponding to strong, medium, weak, and very weak NOEs, respectively (Forman-Kay et al., 1991). Upper distance limits for distances involving methyl protons and nonstereospecifically assigned methylene protons were corrected appropriately for center averaging (Wüthrich et al., 1983), and an additional 0.5 Å was added to the upper limits of NOEs involving methyl groups (Clore et al., 1987; Wagner et al., 1987). Stereospecific assignments and $\phi$, $\psi$, and $\chi_1$ torsion angle restraints were obtained using the conformational grid search program STEREOSEARCH on the basis of the $^3J_{HN\alpha}$ and $^3J_{\alpha\beta}$ coupling constants and the intraresidue and sequential interresidue NOEs involving the NH, $C^\alpha$H, and $C^\beta$H protons (Nilges et al., 1990). The minimum ranges employed for $\phi$, $\psi$, $\chi_1$ torsion angle restraints were ±30°, ±50°, and ±20°, respectively, as described by Kraulis et al. (1989).

Structures were calculated from random starting structures by means of simulated annealing (Nilges et al., 1988a–c). The simulated annealing calculations were carried out using the program XPLOR (Brünger et al., 1986; Brünger, 1990). The target function that is minimized comprises *only* quadratic harmonic potential terms for covalent geometry (i.e., bonds, angles, planes, and chirality), square-well quadratic potentials for the experimental NOE distance and torsion angle restraints, and a quartic van der Waals repulsion term for the nonbonded contacts (Nilges et al., 1988a–c). All peptide bonds were restrained to be trans. Note there are *no* hydrogen bonding, electrostatic, or 6–12 Lennard-Jones empirical potential terms in the target function. The initial starting structures were random (i.e., random in $\phi$ and $\psi$), and the protocol employed involved two stages. The first stage is derived from that described by Nilges et al. (1988a) and represents a minor modification of that given by M. Nilges in the XPLOR Version 2.1 manual (Brünger, 1990). The second stage follows that of the simulated annealing schedule described by Nilges et al. (1988b) with minor modifications given by Kraulis et al. (1989). The zinc can potentially coordinate to the histidines through either the $N^{\delta1}$ or $N^{\epsilon2}$ atoms. As the coordination was not known a priori (except by analogy to previous studies on Cys$_2$His$_2$ zinc fingers), the initial calculations were carried out *without* zinc. These indicated unambiguously that the zinc could only coordinate in a tetrahedral geometry to the $N^{\epsilon2}$ atoms of His-20 and -24 for the N-terminal finger, and His-48 and -54 for the C-terminal finger, in agreement with the findings on other Cys$_2$His$_2$ zinc fingers (Lee et al., 1989; Omichinski et al., 1990; Pavletich & Pabo, 1991). In subsequent calculations, therefore, the zinc atoms were incorporated by introducing appropriate covalent restraints to ensure that the coordination geometry was approximately tetrahedral, that each zinc atom lay in the plane of the two coordinating histidine imidazole rings, that the Cys($C^\beta$)–Cys($S^\gamma$)–Zn and Zn–His($N^{\epsilon2}$)–His($C^{\delta2}/C^{\epsilon1}$) angles were around 107° and 120°, respectively, and that the $S^\gamma$-(Cys)–Zn and $N^{\epsilon2}$(His)–Zn bond lengths had values of 2.3 and 2.0 Å, respectively (Omichinski et al., 1990).

As in previous structure determinations from this laboratory, an iterative strategy was employed (Kraulis et al., 1989; Clore et al., 1990, 1991; Omichinski et al., 1990; Forman-Kay et al., 1991; Gronenborn et al., 1991). At the end of this procedure, stereospecific assignments were obtained for 38 out of the 46 $\beta$-methylene groups, for the methyl groups of the

single Val residue at position 27, and for the two Leu residues at positions 17 and 45. The side chains for the eight residues whose $\beta$-methylene protons were not stereoassigned are disordered about $\chi_1$ as evidenced by $^3J_{\alpha\beta}$ coupling constant values of 6–7 Hz. The final structure calculations were based on a total of 1280 approximate experimental restraints make up of 1135 interproton distance restraints and 145 torsion angle restraints (for 55 $\phi$, 44 $\psi$, and 46 $\chi_1$ angles). The interproton distance restraints were distributed as follows: 528 within the N-terminal zinc finger (residues 1–27), 582 within the C-terminal zinc finger (residues 28–56), and 25 between the two fingers. The coordinates of the simulated annealing structures, together with the experimental NMR restraints, have been deposited in the Brookhaven Protein Data Bank.

## RESULTS AND DISCUSSION

A total of 30 simulated annealing (SA) structures were calculated, and the structural statistics are presented in Table II. The structures of the individual zinc fingers are extremely well-defined (Figures 2–4) with a backbone atomic rms distribution about the mean coordinate positions of 0.32 and 0.33 Å for the N- and C-terminal fingers, respectively. The corresponding values for all atoms, excluding disordered surface side chains, are 0.36 and 0.40 Å. Further, the average angular $\phi$ and $\psi$ rms deviations between the structures are only 9.7 ± 5.4° (residues 3–55) and 9.6 ± 5.5° (residues 2–54), respectively (Figure 3). This reflects the large number of experimental NMR restraints (Clore & Gronenborn, 1991a,b). The stereochemistry of the structures is good as judged by several criteria: all the $\phi,\psi$ angles lie within the allowed regions of a Ramachandran plot, the nonbonded contacts are characterized by a large negative Lennard–Jones van der Waals energy, and the deviations from idealized covalent geometry are small.

There is some degree of uncertainty in the determination of the exact orientation of the two fingers relative to each other. Specifically, the angle between the long axes of the two helices (residues 13–25 and 41–51 from the N- and C-terminal fingers, respectively) adopts a range of values in the calculated SA structures centered around a mean of 47° with a standard deviation of ±5°. This arises from the fact that the double finger is not a globular structure, resulting in relatively few short (<5 Å) interproton distance contacts between the two domains which are detectable by NOE measurements (Table III). Thus, although the backbone $\phi,\psi$ angular rms deviations in the linker region (residues 26–28) connecting the two fingers are less than 5° (Figure 3, Table IV), the small uncertainties in their values are sufficient to give rise to relatively large atomic displacements of one finger relative to the other. This is clearly seen in both Figures 2 and 3 (top two panels), which display superpositions and atomic rms distributions of the 30 SA structures, respectively, when best fitted to either the N- or C-terminal fingers. Nevertheless, only a small average rotation of ~11° about the linker region is required to achieve good superposition of both fingers. Examination of the SA structures reveals that the relative orientation between the two fingers is stabilized by hydrophobic interactions between Thr-23, Val-27, and the methylene groups of Lys-40 and by a hydrogen bond between the $N^\zeta H_3^+$ of Lys-40 and the $O^\gamma H$ of Thr-23 (Figure 6A). As a result, the side chain of Lys-40 is extremely well-defined by a large set of NOEs (see Figure 4B). In addition, a potential hydrogen bond can be formed between the backbone carbonyl of Thr-23 and the guanidinium group of Arg-28. The latter, however, is only present in some of the structures as the guanidinium group of arginine is difficult to observe owing to rapid exchange with water and
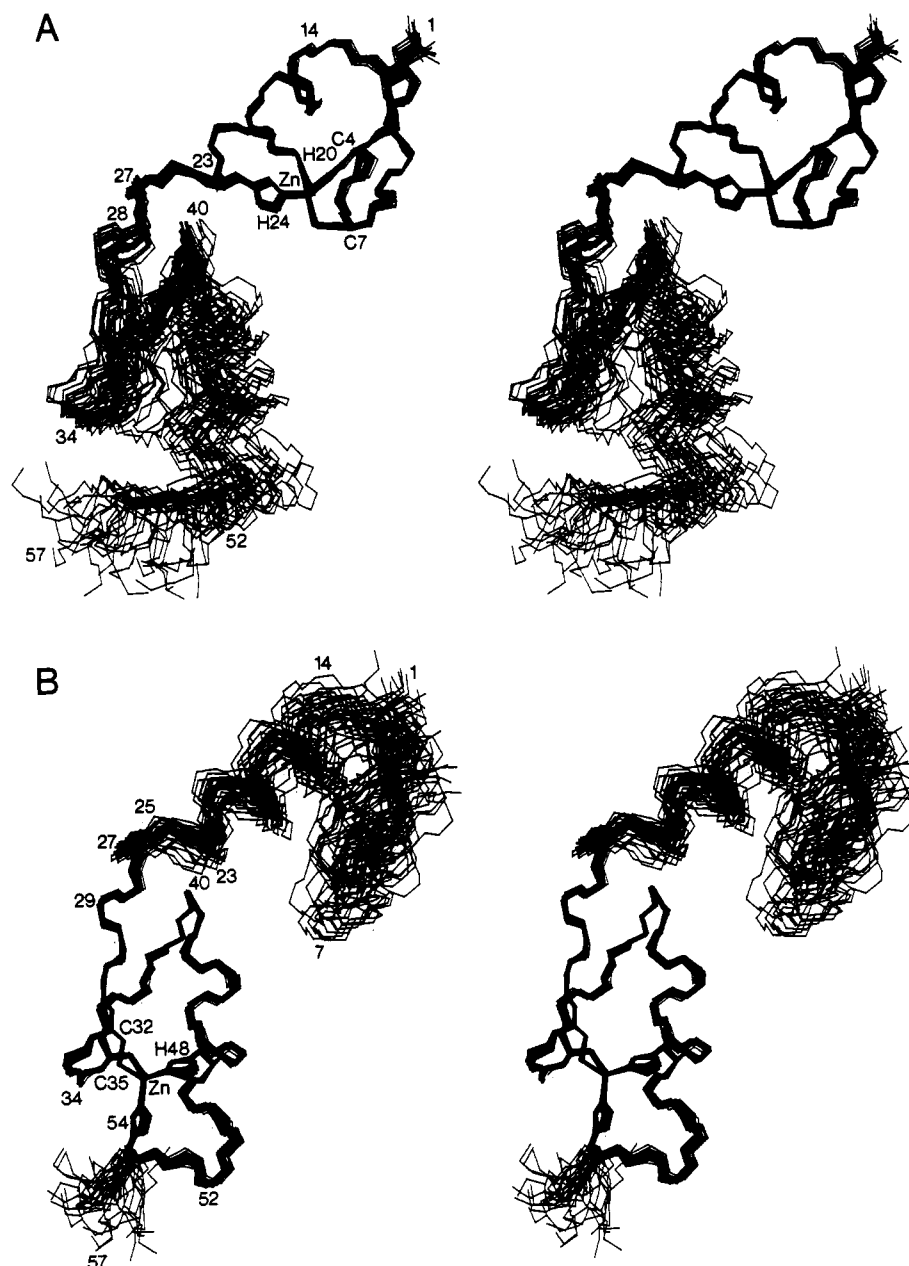
FIGURE 2: Stereoviews showing superpositions of the backbone (N, C$^\alpha$, C) atoms of the 30 SA structures of the double zinc finger of MBP-1 best fitted to (A) the N-terminal finger (residues 2–28) and (B) the C-terminal finger (residues 27–55). The same view is used in (A) and (B).

could therefore not be assigned. Consequently, Arg-28 is only well-defined up to the C$^\delta$ position.

The structural features of the individual fingers are very similar to those reported for small isolated single Cys$_2$His$_2$ zinc finger peptides in solution (Lee et al., 1989; Omichinki et al., 1990; Klevitt et al., 1990; Kochoyan et al., 1991) and to the three fingers of the X-ray structure of the Zif-268–DNA complex (Pavletich & Pabo, 1991). Indeed, in the latter case, the backbone atomic rms differences between the N- and C-terminal fingers of MBP-1 on the one hand and the three fingers of Zif-268 on the other are ∼1.5 and ∼1 Å, respectively. For comparison, the backbone atomic rms difference between the N- and C-terminal fingers of MBP-1 is ∼1.2 Å (for residues 2–24 superimposed on residues 30–52), and that between the three fingers of Zif-268 varies from ∼0.5 to ∼0.9 Å. Each finger comprises an irregular antiparallel β-sheet and hairpin (residues 1–12, 28–40) and a single helix (residues 13–25, 41–51). The zinc is coordinated in a tetrahedral fashion

to the S$^\gamma$ atoms of the two cysteines (Cys-4 and -7, Cys-32 and -35) located in the antiparallel β-sheet and to the N$^{\epsilon 2}$ atoms of two histidines (His-20 and -24, His-48 and -54). In the case of the N-terminal finger where the histidines are separated by three residues, both histidines are located along the helix (Figure 2A and 4A). In the C-terminal finger, on the other hand, the histidines are separated by five residues and the helix stops at position 51, leading into a looplike structure which serves to correctly position His-54 for tetrahedrally coordinating to the zinc atom (Figures 2B and 4B). The fingers are stabilized not only by the zinc coordination but also by a tightly packed hydrophobic core which comprises Tyr-2, Ile-9, Abu-11 (which replaces the cysteine of the native protein; Sakaguchi et al., 1991), Leu-17, and Ile-21 in the N-terminal finger (Figure 4A) and by the corresponding residues Tyr-30, Phe-37, Phe-39, Leu-45, and Met-49 in the C-terminal finger (Figure 4B).

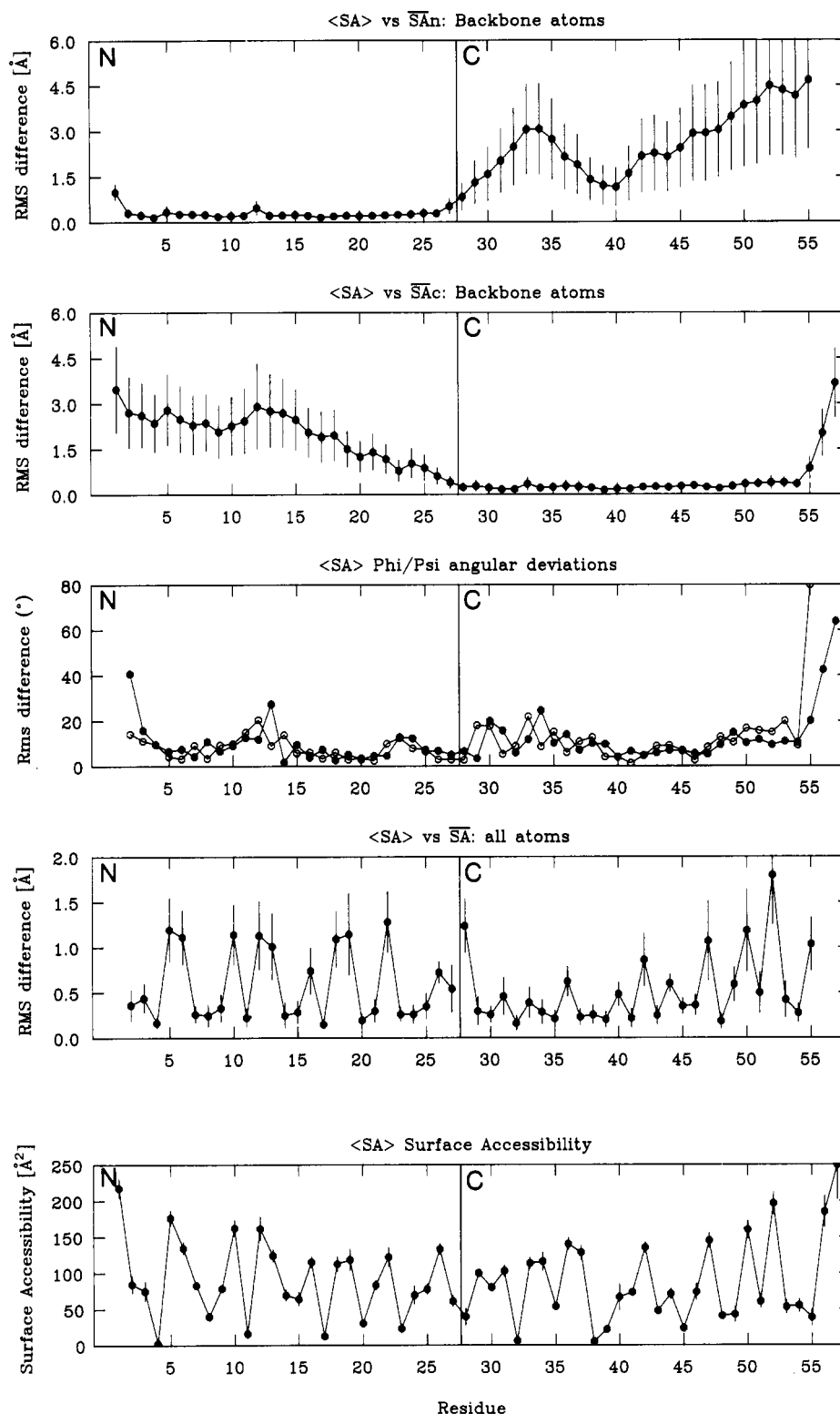Comparison of the double zinc finger of MBP-1 with the

FIGURE 3: Atomic rms distribution about the mean coordinate positions, angular rms deviations, and surface accessibility, as a function of residue number for the 30 SA structures of MBP-1. The first and second panels display the backbone atomic rms distribution about the mean coordinate positions obtained by best fitting the individual SA coordinates to the N-(residues 2–28; $\overline{SA}n$) and C- (residues 27–55; $\overline{SA}c$) terminal zinc fingers, respectively. The third panel shows the angular rms deviations for the $\phi$ and $\psi$ backbone torsion angles as closed (●) and open (○) circles, respectively. The atomic rms distribution for all atoms is shown in the fourth panel, and the values for the N- and C-terminal halves are obtained separately by best fitting to residues 2–28 and 27–55, respectively. The fifth panel displays the surface accessibilities. The symbols represent the average values and the vertical lines their standard deviations.

triple zinc finger of Zif-268 in its complex with DNA (Pavletich & Pabo, 1991) reveals that the orientation of the zinc fingers relative to each other is quite different in the two cases. This is illustrated by the two sets of superpositions and the schematic ribbon drawings shown in Figures 5 and 6, respectively. In the first superposition, the N-terminal finger of MBP-1 and finger 2 of the finger 2–3 segment of Zif-268 are superimposed on finger 1 of the finger 1–2 segment of Zif-268 (Figure 5A), while in the second the C-terminal finger of MBP-1 and finger 3 of the finger 2–3 segment of Zif-268

Table II: Structural Statistics and Atomic rms Differences[a]

| structural statistics | $\langle SA \rangle$ |
|---|---|
| RMS deviations from exptl interproton distance restraints (Å)[b] | |
| all (1135) | 0.026 ± 0.001 |
| N-terminal finger (residues 1–27) (528) | |
| interresidue sequential ($|i - j| = 1$) (100) | 0.024 ± 0.002 |
| interresidue short range ($1 < |i - j| \leq 5$) (131) | 0.035 ± 0.003 |
| interresidue long range ($|i - j| > 5$) (116) | 0.033 ± 0.002 |
| intraresidue (181) | 0.036 ± 0.002 |
| C-terminal finger (residues 28–57) (582) | |
| interresidue sequential ($|i - j| = 1$) (131) | 0.009 ± 0.003 |
| interresidue short range ($1 < |i - j| \leq 5$) (105) | 0.012 ± 0.002 |
| interresidue long range ($|i - j| > 5$) (138) | 0.019 ± 0.003 |
| intraresidue (208) | 0.022 ± 0.002 |
| Interdomain (25) | |
| sequential ($|i - j| = 1$) (5)[c] | 0.011 ± 0.009 |
| short range ($1 < |i - j| \leq 5$) (6) | 0.060 ± 0.014 |
| interresidue long range ($|i - j| > 5$) (14) | 0.028 ± 0.010 |
| RMS deviations from exptl dihedral restraints (deg) (145)[b,d] | 0.140 ± 0.035 |
| $F_{NOE}$ (kcal·mol⁻¹)[e] | 23.9 ± 1.6 |
| $F_{tor}$ (kcal·mol⁻¹)[e] | 0.18 ± 0.08 |
| $F_{repel}$ (kcal·mol⁻¹)[e] | 18.0 ± 1.3 |
| $E_{L-J}$ (kcal·mol⁻¹)[f] | −173.3 ± 5.5 |
| deviations from idealized covalent geometry[g] | |
| bonds (Å) (980) | 0.005 ± 0 |
| angles (deg) (1789) | 1.869 ± 0.002 |
| impropers (deg) (402)[h] | 0.989 ± 0.007 |

| | atomic rms differences (Å) | |
|---|---|---|
| | $\langle SA \rangle$ vs $\overline{SAn}$ N-terminal finger (residues 2–28) | $\langle SA \rangle$ vs $\overline{SAc}$ C-terminal finger (residues 27–55) |
| backbone atoms | 0.32 ± 0.09 | 0.33 ± 0.07 |
| all atoms | 0.81 ± 0.06 | 0.69 ± 0.08 |
| all atoms excluding disordered side chains[i] | 0.36 ± 0.09 | 0.40 ± 0.06 |

[a] The notation of the structures is as follows: $\langle SA \rangle$ are the 30 simulated annealing structures; $\overline{SAn}$ and $\overline{SAc}$ are the mean coordinate positions obtained by best fitting all 30 SA structures to the N-terminal finger (residues 2–28) and to the C-terminal finger (residues 27–55), respectively. The number of terms for the various restraints is given in parentheses. [b] None of the structures exhibit distance violations greater than 0.3 Å or dihedral angle violations greater than 1°. [c] The sequential ($|i - j| = 1$) interdomain NOEs involve contacts between residues 27 and 28. [d] The torsion angle restraints comprise 55 $\phi$, 44 $\psi$, and 45 $\chi_1$ angles. [e] The values of the square-well NOE ($F_{NOE}$) and torsion angle ($F_{tor}$) potentials [cf. eqs 2 and 3 in Clore et al. (1986)] are calculated with force constants of 50 kcal·mol⁻¹·Å⁻² and 200 kcal·mol⁻¹·rad⁻², respectively. The value of the quartic van der Waals repulsion term $F_{rep}$ [cf. eq 5 in Nilges et al. (1988b)] is calculated with a force constant of 4 kcal·mol⁻¹·Å⁻⁴ with the hard-sphere van der Waals radii set to 0.8 times their standard values in the CHARMM empirical energy function (Brooks et al., 1983). [f] $E_{L-J}$ is the Lennard–Jones van der Waals energy calculated with the CHARMM (Brooks et al., 1983) empirical energy function and is *not* included in the target function for simulated annealing or restrained minimization. [g] These include terms for the tetrahedral coordination geometry of the two zinc atoms which are each bonded to the S$^\gamma$ atoms of two cysteines and the N$^{\epsilon 2}$ atoms of two histidines (Omichinski et al., 1990). [h] The improper torsion restraints serve to maintain planarity and chirality. [i] The disordered surface side chains which have been excluded are as follows: in the N-terminal finger, Glu-5 from the C$^\delta$ position onward, Glu-6 from C$^\delta$, Arg-10 from C$^\delta$, Lys-12 from C$^\delta$, Lys-13 from C$^\delta$, Met-16 from S$^\delta$, Lys-18 from C$^\gamma$, Lys-19 from C$^\gamma$, Arg-22 from C$^\delta$, Asp-26 from C$^\gamma$, and Arg-28 from N$^\epsilon$; in the C-terminal finger, Arg-28 from N$^\epsilon$, Asn-36 from C$^\gamma$, Lys-42 from C$^\delta$, Asn-44 from C$^\gamma$, Lys-47 from C$^\gamma$, Lys-50 from C$^\delta$, Lys-52 from C$^\gamma$, and Ser-55 O$^\gamma$.

are superimposed on finger 2 of the finger 1–2 segment of Zif-268 (Figure 5B). Only slight differences are seen in the relative orientations of adjacent Zif-268 fingers. The magnitude of these differences is not much smaller than the variation in relative orientation between the N- and C-terminal fingers of MBP-1 observed within the set of 30 SA structures (Figure 2). The relative orientation, however, of the N- and C-terminal fingers of MBP-1 is distinctly different from that seen in the Zif-268 fingers. The transformation required to best fit the N-terminal finger of MBP-1 to finger 1 of Zif-268 from a coordinate set of 30 SA structures in which the C-

terminal finger is best fitted to finger 2 of Zif-268 involves a rotation of 74 ± 11° about the linker region; the corresponding value with regard to the finger 2–3 segment of Zif-268 is 96 ± 11°. This can be readily appreciated from the schematic ribbon drawings shown in Figure 6 in which the C-terminal finger of MBP-1 and finger 2 of Zif-268 are viewed in the same orientation. In this view, the long axis of the helix of the N-terminal finger of MBP-1 lies in the plane of the paper (Figure 6A), while that of finger 1 of Zif-268 is directed into the plane of the paper at an angle of about 60° (Figure 6B). At the same time, the long axis of the antiparallel sheet in the N-terminal finger of MBP-1 lies approximately parallel to the long axis of the helix of the C-terminal finger (Figure 6A), whereas the long axis of the antiparallel sheet of finger 1 in Zif-268 lies approximately perpendicular to the long axis of the helix of finger 2 (Figure 6B).

This finding was further investigated by examining short (<5 Å) interproton contacts (i.e., those in principle observable by NMR) between the zinc fingers of MBP-1 and Zif-268. While such contacts are seen between Val-27 and Lys-40 and between Thr-23 and Phe-39, Lys-40, and Thr-41 in MBP-1 (Figure 6A), the equivalent contacts in Zif-268 are all greater than 5 Å. Further, in Zif-268, contacts exist between residues at positions 22 and 40, using the numbering scheme of MBP-1 (Figure 6B). Whereas the fingers of both MBP-1 and Zif-268 contain the same amino acid at position 22, namely, Arg, the residues at positions equivalent to 40 in fingers 2 and 3 of Zif-268, namely, Ser and Ala, have much smaller side chains, and the orientation of the two domains is stabilized by a hydrogen bond between the guanidinium group of the arginine at position 22 and the backbone carbonyl of the residue at position 40 (Pavletich & Pabo, 1991). Such a hydrogen bond cannot occur in MBP-1 owing to steric interference by the long Lys side chain at position 40.

Interestingly, most of the $\phi$ and $\psi$ backbone torsion angles in the linker region and the immediately adjacent residues (i.e., residues 25–30) are not significantly different in MBP-1 and Zif-268 (Table IV). This is hardly surprising as only small changes in these angles are required to produce large changes in the relative orientations of the fingers. The only major difference lies in the $\phi$ angle of residue 26 whose value is negative (−150°) for the Asp in MBP-1 but positive (+80°) for the Gly in Zif-268 and is compensated by appropriate changes in the values of the $\psi$ torsion angles of the two adjacent residues. It is important to note that the different value of $\phi$ for residue 26 is not per se responsible for the different relative orientations of the fingers in the two proteins. Thus, if one artificially restrains the $\phi$ angle of Asp-26 to be positive and removes the $\psi$ restraints on the two adjacent residues, the orientation of the two fingers of MBP-1 in the resulting calculated structures remains unchanged.

The different orientation of the fingers in MBP-1 compared to that observed in Zif-268 has a number of important consequences with respect to specific DNA binding. In particular, if either one of the fingers of MBP-1 is superimposed on any one of the Zif-268 fingers in the Zif-268–DNA complex, the other finger cannot contact the DNA. Three possible scenarios can be deduced for binding of MBP-1 to DNA. First, the orientation of the fingers in MBP-1 may change upon binding so that they adopt the same relative orientation as that observed in the Zif-268 complex with DNA. We feel that this is probably unlikely owing to the presence of the long Lys-40 side chain as described above and would necessitate a substantial conformational change. In this regard, it is interesting to note that mutation of a Thr to the more bulky Ile at the
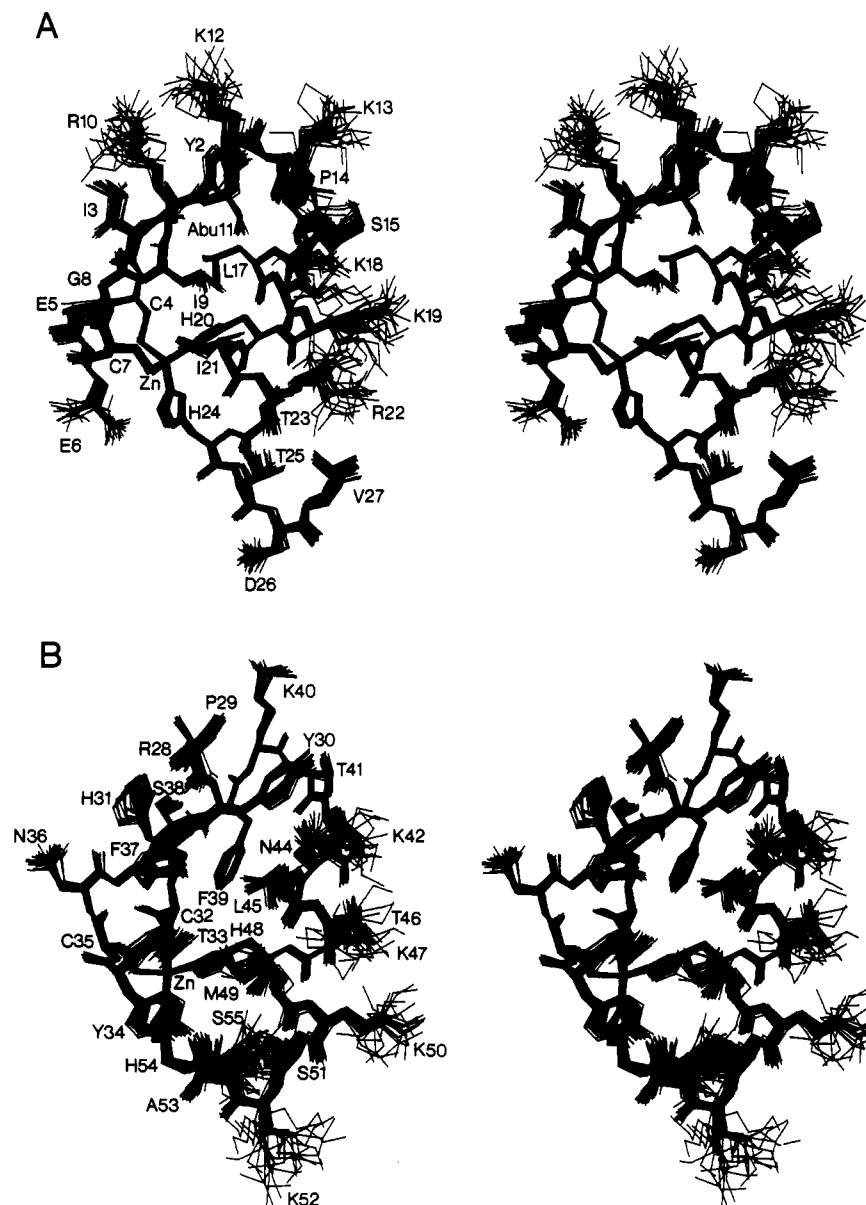
FIGURE 4: Stereoviews showing best fit superpositions of all atoms (excluding protons) of the 30 SA structures for the N- (A) and C- (B) terminal zinc fingers of MBP-1. For clarity, the side chains of Glu-5 in (A) and Arg-28 in (B) are only shown up to the $C^\beta$ and $C^\delta$ positions, respectively, as they are not defined beyond these positions by the experimental data.

Table III: Summary of the Interdomain NOEs Observed between the N- (Residues 1–27) and C- (Residues 28–57) Terminal Fingers of MBP-1[a]

| | | |
|---|---|---|
| sequential NOEs ($|i - j| = 1$) | | |
| V27(NH)–R28(NH)w | V27($C^\alpha$H)–R28(NH) s | V27($C^\beta$H)–R28(NH) w |
| V27($C^{\gamma 2}H_3$)–R28(NH) m | V27($C^{\gamma 2}H_3$)–R28($C^\alpha$H) w | |
| short-range NOEs ($1 < |i - j| \le 5$) | | |
| T23($C^\alpha$H)–R28(NH) w | T23($C^\alpha$H)–R28(N$^\epsilon$H) w | T23($C^{\gamma 2}H_3$)–R28(NH) w |
| V27($C^{\gamma 2}H_3$)–P29($C^{\delta 1}$H) m | V27($C^{\gamma 2}H_3$)–P29($C^{\delta 2}$H) m | V27($C^{\gamma 2}$H3)–P29($C^\gamma$H) w |
| long-range NOEs ($|i - j| > 5$) | | |
| T23($C^{\gamma 2}H_3$)–F39($C^\alpha$H) w | T23($C^{\gamma 2}H_3$)–K40(NH) w | T23($C^{\gamma 2}H_3$)–K40($C^\alpha$H) w |
| T23($C^{\gamma 2}H_3$)–K40($C^{\beta 3}$H) m | T23($C^{\gamma 2}H_3$)–K40($C^{\beta 2}$H) m | T23($C^{\gamma 2}H_3$)–K40($C^\gamma$H) m |
| T23($C^{\gamma 2}H_3$)–K40($C^\delta$H) w | T23($C^{\gamma 2}H_3$)–K40($C^\epsilon$H) w | T23($C^{\gamma 2}H_3$)–T41($C^{\gamma 2}H_3$) w |
| V27($C^\alpha$H)–K40($C^\delta$H) w | V27($C^\beta$H)–K40($C^\epsilon$H) w | V27($C^{\gamma 1}H_3$)–K40($C^\epsilon$H) w |
| V27($C^{\gamma 2}H_3$)–K40($C^\delta$H) w | V27($C^{\gamma 2}H_3$)–K40($C^\epsilon$H) w | |

[a] The NOE intensities are indicated as strong (s), medium (m), or weak (w).

equivalent position in the double zinc finger of ADR1 significantly reduces its ability to activate transcription (Blumberg et al., 1987), while replacement of this Thr by the smaller Ala has no effect (Thukral et al., 1991). This further supports the importance of the residue at position 40 (current numbering scheme) in determining the relative orientation of the fingers and hence the mode of DNA binding. It also implies that

ADR1 and Zif-268 bind to DNA in a similar manner and leads one to the second possibility that MBP-1 may bind to its DNA target site in a mode quite different from that observed for Zif-268. Indeed, our modeling studies indicate that one can position the helices of MBP-1 into the major groove covering approximately 10 base pairs, consistent with the results of methylation protection and interference experiments
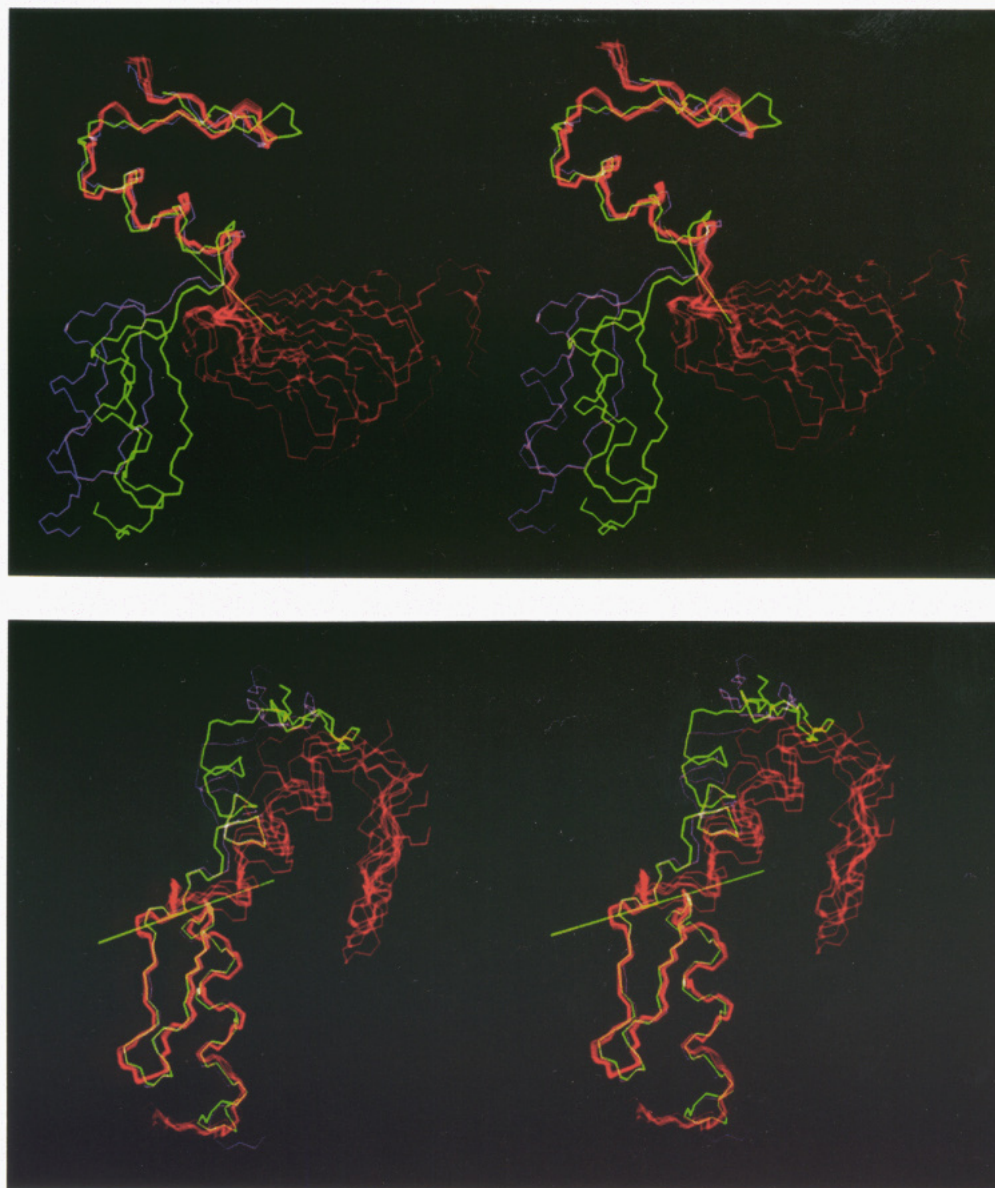
FIGURE 5: Two different stereoviews showing superpositions of the zinc fingers from the X-ray structure of the Zif-268–DNA complex (Pavletich & Pabo, 1991) and of five SA structures of MBP-1. The finger 1–2 and 2–3 segments of the X-ray structure of Zif-268 are shown in green and magenta, respectively, while the five SA structures of MBP-1 are shown in red. (A, top) The N-terminal zinc finger of the five SA structures and finger 2 of the finger 2–3 segment of Zif-268 (magenta) are best fitted to finger 1 of the finger 1–2 segment (green) of Zif-268. (B, bottom) The C-terminal zinc finger of the five SA structures and finger 3 of the finger 2–3 segment (magenta) of Zif-268 are best fitted to finger 2 of the finger 1–2 segment (green) of Zif-268. For clarity, the views shown in (A) and (B) are different. The five SA structures shown have been selected from the set of 30 to display the full range of relative orientations of the N- and C-terminal fingers observed in MBP-1 and to demonstrate that this divergence occurs in a direction different from that seen between the MBP-1 and Zif-268 fingers. Thus, one can readily see in (B) that the long axis of the antiparallel sheet of the N-terminal finger is approximately parallel to the long axis of the helix of the adjacent C-terminal finger in all the SA structures of MBP-1, in contrast to the situation in Zif-268 where it is approximately perpendicular. The approximate location of the axis of rotation required to transform the coordinates from a set in which the N-terminal finger of MBP-1 is best fitted to finger 1 of MBP-1 to one in which the C-terminal finger of MBP-1 is best fitted to finger 2 of MBP-1, and vice versa, is indicated by a straight yellow line. (Note that finger 1, shown in green, of Zif-268 has four residues between the two cysteines which are coordinated to zinc, whereas the other fingers only have two residues in this location.)

(Clark et al., 1990; Fan & Maniatis, 1990). For straight classical B-DNA this would position the two helices differently with respect to the long axis of the DNA. Finally, if both helices adopt similar orientations with regard to the DNA, bending of the DNA would have to take place. This is not unprecedented and has been observed previously in other DNA–protein complexes (Wu & Crothers, 1984; Schultz et al., 1991; Brennan et al., 1990).

In summary, while the structures of the individual zinc fingers of MBP-1 are very similar to those of other classical Cys$_2$His$_2$ fingers (Lee et al., 1989; Omichinski et al., 1990; Klevitt et al., 1990; Kochoyan et al., 1991a–c), the orientation

of the two fingers in the free uncomplexed state is markedly different from that observed in the triple zinc finger of Zif-268 in its complex with DNA (Pavletich & Pabo, 1991). As discussed above, this implies that the mode of contact with DNA in MBP-1 may well be distinct from that observed in the Zif-268 complex. This is supported by the fact that, in the case of Zif-268, the three fingers contact a total of 9 base pairs as deduced from both the crystal structure of the complex (Pavietich & Pabo, 1991) and methylation interference experiments (Christy & Nathans, 1989), while in the case of MBP-1, methylation interference experiments reveal that binding involves a symmetrical region of ~10 base pairs

Table IV: Experimental $\phi,\psi$ Torsion Angle Restraints and $\phi,\psi$ Values in the SA Structures of the Linker Region (Residues 25–30) Connecting the N- and C-Terminal Fingers of MBP-1, Together with the Corresponding Values Found in the Crystal Structure of the Triple Zinc Fingers of Zif-268 Complexed with DNA

| $\phi$ backbone torsion angles (deg) | | | | | | |
|---|---|---|---|---|---|---|
| MBP-1 | T25 | D26 | V27 | R28 | P29 | Y30 |
| exptl restraints[a] | $-70 \pm 50$ | $-115 \pm 60$ | $-90 \pm 70$ | $-110 \pm 50$ | $-70 \pm 30$ | $-100 \pm 50$ |
| $\langle SA \rangle$ structures[b] | $-94 \pm 5$ | $-154 \pm 5$ | $-97 \pm 4$ | $-120 \pm 5$ | $-63 \pm 3$ | $-78 \pm 14$ |
| fingers 1–2 of Zif-268[c] | T | G | Q | K | P | F |
| | $-81$ | $78$ | $-66$ | $-127$ | $-60$ | $-116$ |
| fingers 2–3 of Zif-268[c] | T | G | E | K | P | F |
| | $-78$ | $80$ | $-78$ | $-134$ | $-73$ | $-114$ |
| $\psi$ backbone torsion angles (deg) | | | | | | |
| MBP-1 | T25 | D26 | V27 | R28 | P29 | Y30 |
| exptl restraints[a] | $-30 \pm 90$ | $-10 \pm 100$ | $80 \pm 90$ | $80 \pm 50$ | $-15 \pm 50$ | $110 \pm 50$ |
| $\langle SA \rangle$ structures[b] | $-105 \pm 5$ | $29 \pm 2$ | $46 \pm 2$ | $85 \pm 2$ | $-24 \pm 13$ | $93 \pm 12$ |
| fingers 1–2 of Zif-268[c] | T | G | Q | K | P | F |
| | $-17$ | $6$ | $120$ | $77$ | $-8$ | $122$ |
| fingers 2–3 of Zif-268[c] | T | G | E | K | P | F |
| | $-27$ | $19$ | $133$ | $92$ | $-13$ | $116$ |

[a] The experimental $\phi,\psi$ torsion angle restraints are obtained using the conformational grid search program STEREOSEARCH on the basis of the $^3J_{NH\alpha}$ and $^3J_{\alpha\beta}$ coupling constants and the intraresidue and sequential interresidue NOEs involving the NH, $C^\alpha$H, and $C^\beta$H protons (Nilges et al., 1990). The minimum ranges employed for the $\phi$ and $\psi$ restraints are $\pm30°$ and $\pm50°$, respectively, and the torsion angle restraints are described by a square-well potential [cf. eq 3 of Clore et al. (1986)]. The measured values of the $^3J_{HN\alpha}$ coupling constants for Thr-25, Asp-26, Val-27, Arg-28, and Tyr-30 are 8, 8, 8, 9, and 7 ($\pm1.5$) Hz, respectively. [b] These values are the averages obtained for the 30 calculated SA structures. Note that the spread of the $\phi,\psi$ torsion angles in the linker region of the SA structures is very much smaller than the width of the experimental restraints. The reason that these $\phi,\psi$ angles are so well-defined in the SA structures can be attributed to the nonsequential NOEs. [c] From Pavletich and Pabo (1991).
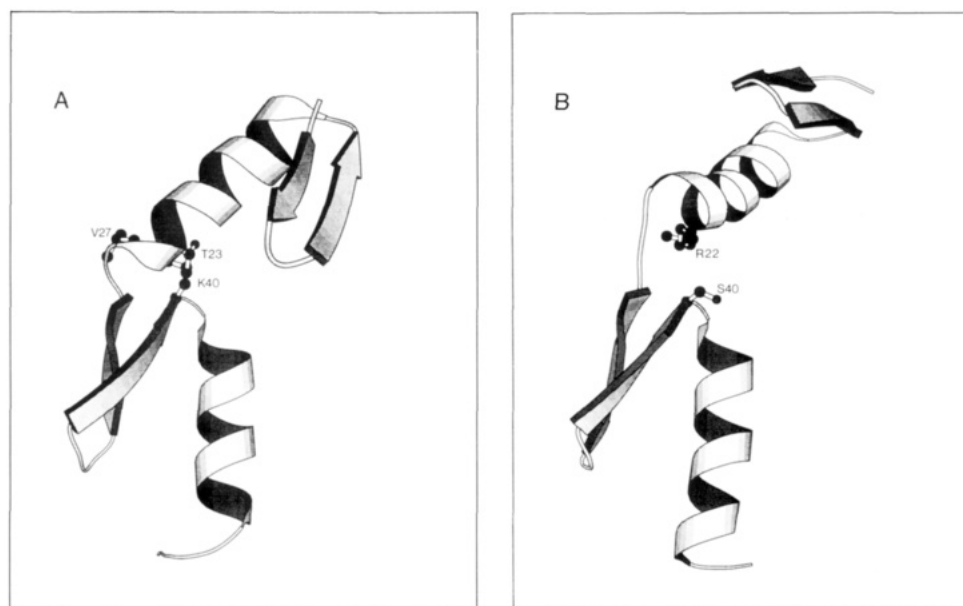


FIGURE 6: Schematic ribbon drawing of the zinc fingers of MBP-1 (A) and fingers 1 and 2 of Zif-268 (B). In the view displayed, the C-terminal finger of MBP-1 and finger 2 of Zif-268 are shown in the same orientation. Side chains involved in interdomain contacts are shown, and the residue numbering used for Zif-268 follows that of MBP-1. The program Molscript (Kraulis, 1991) was used to create the ribbon drawings, and the coordinates of Zif-268 are from Pavletich and Pabo (1991).

(Clark et al., 1990; Fan & Maniatis, 1990). Moreover, the conserved Arg, Asp, and Arg residues at positions 13/41, 15/43, and 19/47 (numbering scheme of MBP-1) in the Zif-268 zinc fingers which are involved in hydrogen-bonding interactions with the DNA bases are substituted by Lys/Thr, Ser/Gly, and Lys in the MBP-1 zinc fingers. The present result therefore suggests that the simple rules (Klevitt, 1991) derived from the interactions observed in the Zif-268–DNA complex (Pavletich & Pabo, 1991) cannot necessarily be transferred to other systems. Indeed, it seems likely that the variety of different orientations adopted by the recognition helices of the helix–turn–helix family of DNA binding proteins (Steitz, 1990) will also be found for the Cys$_2$His$_2$ zinc finger proteins. Structural studies on the double zinc finger MBP-1–DNA complex by NMR have been initiated to further investigate this issue.

REFERENCES

Baldwin, A. S., LeClair, K. P., Singh, H., & Sharp, P. A. (1990) *Cell Biol. 10*, 1046.

Bax, A. (1989) *Methods Enzymol. 176*, 151.

Berg, J. M. (1990) *Annu. Rev. Biophys. Biophys. Chem. 19*, 405.

Blumberg, J., Eisen, A., Sledgziewski, Bader, D., & Young, E. T. (1987) *Nature 328*, 443.

Brennan, R. G., Roderick, S. L., Takeda, Y., & Matthews, B. W. (1990) *Proc. Natl. Acad. Sci. U.S.A. 87*, 8165.

Brooks, B. R., Bruccoleri, R. E., Olafson, B. D., States, D. J., Swaminathan, S., & Karplus, M. (1983) *J. Comput. Chem. 4*, 187.

Brown, R. S., Sander, C., & Argos, P. (1985) *FEBS Lett. 186*, 271.

Brünger, A. T. (1990) *XPLOR Version 2.1 Manual*, Yale University, New Haven, CT.

Brünger, A. T., Clore, G. M., Gronenborn, A. M., & Karplus, M. (1986) *Proc. Natl. Acad. Sci. U.S.A. 83*, 3801.

Christy, B., & Nathans, D. (1989) *Proc. Natl. Acad. Sci. U.S.A. 86*, 8737.

Clark, L., Matthews, J. R., & Hay, R. T. (1990) *J. Virol. 64*, 1335.

Clore, G. M., & Gronenborn, A. M. (1987) *Protein Eng. 1*, 275.

Clore, G. M., & Gronenborn, A. M. (1989) *CRC Crit. Rev. Biochem. Mol. Biol. 24*, 479.

Clore, G. M., & Gronenborn, A. M. (1991a) *Annu. Rev. Biophys. Biophys. Chem. 20*, 29.

Clore, G. M., & Gronenborn, A. M. (1991b) *Science 252*, 1390.

Clore, G. M., Nilges, M., Sukumaran, D. K., Brünger, A. T., Karplus, M., & Gronenborn, A. M. (1986) *EMBO J. 5*, 2729.

Clore, G. M., Gronenborn, A. M., Nilges, M., & Ryan, C. (1987) *Biochemistry 26*, 8012.

Clore, G. M., Appella, E., Yamada, M., Matsushima, K., & Gronenborn, A. M. (1990) *Biochemistry 29*, 1689.

Clore, G. M., Wingfield, P. T., & Gronenborn, A. M. (1991) *Biochemistry 30*, 2315.

Ernst, R. R., Bodenhausen, G., & Wokaun, A. (1987) *Principles of Nuclear Magnetic Resonance in One and Two Dimensions*, Clarendon Press, Oxford, U.K.

Fan, C. M., & Maniatis, T. (1990) *Genes Dev. 4*, 2119.

Forman-Kay, J. D., Clore, G. M., Wingfield, P. T., & Gronenborn, A. M. (1991) *Biochemistry 30*, 2685.

Gibson, T. J., Postma, J. P. M., Brown, R. S., & Argos, P. (1988) *Protein Eng. 2*, 209.

Gronenborn, A. M., Filpula, D. R., Essig, N. Z., Achari, A., Whitlow, M., Wingfield, P. T., & Clore, G. M. (1991) *Science 253*, 657.

Jeener, J., Meier, B. H., Bachmann, P., & Ernst, R. R. (1979) *J. Chem. Phys. 71*, 4546.

Klevitt, R. E. (1991) *Science 253*, 1367.

Klevitt, R. E., Herriott, J. R., & Horvath, S. J. (1990) *Proteins: Struct., Funct., Genet. 7*, 215.

Klug, A., & Rhodes, D. (1987) *Trends Biochem. Sci. 12*, 464.

Kochoyan, M., Havel, T. F., Nguyen, D., Dahl, C. E., Keutmann, H. T., & Weiss, M. A. (1991a) *Biochemistry 30*, 3371.

Kochoyan, M., Keutmann, H. T., & Weiss, M. A. (1991b) *Biochemistry 30*, 7063.

Kochoyan, M., Keutmann, H. T., & Weiss, M. A. (1991c) *Proc. Natl. Acad. Sci. U.S.A. 88*, 8455.

Kraulis, P. J. (1991) *J. Appl. Crystallogr. 24*, 946.

Kraulis, P. J., Clore, G. M., Nilges, M., Jones, T. A., Pettersson, G., Knowles, J., & Gronenborn, A. M. (1989) *Biochemistry 28*, 7241.

Lee, M. S., Gippert, G. P., Soman, K. V., Case, D. A., & Wright, P. E. (1989) *Science 245*, 653.

Maekawa, T., Sakura, H., Sudo, T., & Ishii, S. (1989) *J. Biol. Chem. 264*, 14591.

Marion, D., & Bax, A. (1988) *J. Magn. Reson. 80*, 528.

Miller, J., McLachlan, A. D., & Klug, A. (1985) *EMBO J. 4*, 1609.

Mueller, L. (1987) *J. Magn. Reson. 72*, 191.

Neuhaus, D., Nakaseko, Y., Nagai, K., & Klug, A. (1990) *FEBS Lett. 262*, 179.

Nilges, M., Gronenborn, A. M., Brünger, A. T., & Clore, G. M. (1988a) *Protein Eng. 2*, 27.

Nilges, M., Clore, G. M., & Gronenborn, A. M. (1988b) *FEBS Lett. 229*, 317.

Nilges, M., Clore, G. M., & Gronenborn, A. M. (1988c) *FEBS Lett. 239*, 129.

Nilges, M., Clore, G. M., & Gronenborn, A. M. (1990) *Biopolymers 29*, 813.

Omichinski, J. G., Clore, G. M., Appella, E., Sakaguchi, K., & Gronenborn, A. M. (1990) *Biochemistry 29*, 9324.

Parraga, G., Horvath, S. J., Eisen, A., Taylor, W. E., Hood, L., Young, E. T., & Klevitt, R. E. (1988) *Science 241*, 1489.

Pavletich, N. P., & Pabo, C. O. (1991) *Science 252*, 809.

Sakaguchi, K., Appella, E., Omichinski, J. G., Clore, G. M., & Gronenborn, A. M. (1991) *J. Biol. Chem. 266*, 7306.

Schultz, S. C., Shields, G. C., & Steitz, T. A. (1991) *Science 253*, 1001.

Singh, H., LeBowitz, J. H., Baldwin, A. S., & Sharp, P. A. (1988) *Cell 52*, 415.

Steitz, T. A. (1990) *Q. Rev. Biophys. 23*, 205.

Thukral, S. K., Morrison, M. L., & Young, E. T. (1991) *Proc. Natl. Acad. Sci. U.S.A. 88*, 9188.

Wagner, G., Braun, W., Havel, T. F., Schaumann, T., Go, N., & Wüthrich, K. (1987) *J. Mol. Biol. 196*, 611.

Wu. H.-M., & Crothers, D. M. (1984) *Nature 308*, 509.

Wüthrich, K. (1986) *NMR of Proteins and Nucleic Acids*, John Wiley, New York.

Wüthrich, K. (1989) *Acc. Chem. Res. 22*, 36.

Wüthrich, K., Billetter, M., & Braun, W. (1983) *J. Mol. Biol. 169*, 949.

Xu, R. X., Horvath, S. J., & Klevitt, R. E. (1991) *Biochemistry 30*, 3371.